

# Prediction of A2 to B2 Phase Transition in the High-Entropy Alloy Mo-Nb-Ta-W

WILLIAM PAUL HUHN<sup>1,2</sup> and MICHAEL WIDOM<sup>1,3</sup>

1.—Carnegie Mellon University, Pittsburgh, PA 15213, USA. 2.—e-mail: wph@andrew.cmu.edu.  
3.—e-mail: widom@andrew.cmu.edu

In this article, we show that an effective Hamiltonian fit with first-principles calculations predicts that an order/disorder transition occurs in the high-entropy alloy Mo-Nb-Ta-W. Using the Alloy Theoretic Automated Toolkit, we find  $T = 0$  K enthalpies of formation for all binaries containing Mo, Nb, Ta, and W, and in particular, we find the stable structures for binaries at equi-atomic concentrations are close in energy to the associated B2 structure, suggesting that at intermediate temperatures, a B2 phase is stabilized in Mo-Nb-Ta-W. Our previously published hybrid Monte Carlo (MC)/molecular dynamics (MD) results for the Mo-Nb-Ta-W system are analyzed to identify certain preferred chemical bonding types. A mean field free energy model incorporating nearest-neighbor bonds is derived, allowing us to predict the mechanism of the order/disorder transition. We find the temperature evolution of the system is driven by strong Mo-Ta bonding. A comparison of the free energy model and our MC/MD results suggests the existence of additional low-temperature phase transitions in the system likely ending with phase segregation into binary phases.

## INTRODUCTION

Alloys of four or more constituent chemical species, each having roughly equal concentration, are known as high entropy alloys (HEAs). Two properties of HEAs justify research interest in the topic. The first, relevant to material design, is that these alloys exhibit a cocktail effect,<sup>1</sup> whereby the selection of individual constituent species tunes various material properties of the alloys. The second, relevant to material growth and theoretical modeling, is that simple lattices are stabilized at moderate and high temperatures. For a solid solution of  $N$  species, each of concentration  $1/N$ , the high-temperature entropy limit is  $k_B \ln N$ . Because all atomic species play equivalent roles, body-centered cubic (bcc) and face-centered cubic (fcc) phases form rather than complex intermetallic phases.<sup>2,3</sup> Experimentally, many samples consist of a single simple phase, and those with multiple phase regions contain simple phases like A2 (bcc) and B2 (CsCl) rather than complex intermetallic structures. This greatly simplifies theoretical modeling, as simple bcc and fcc models with ideal entropy may be used to understand the thermodynamic stability of these materials.

One research focus of HEAs is on alloys containing the refractory metals Mo, Nb, Ta, and W. These species are notable for their high melting temperatures, between 2750 K and 3695 K. Alloying may be used to increase the melting temperature of HEAs, which has the added effect of increasing the onset temperature of alloy softening, which occurs around 50–60% of melting temperature. Additionally, atomic radius mismatch creates localized distortions in the lattice, inducing solid-solution strengthening.<sup>2,4</sup> High melting temperatures and strong mechanical properties make these HEAs useful for aerospace and other applications. Previous experimental work in Mo-Nb-Ta-W and Mo-Nb-Ta-V-W<sup>5,6</sup> shows single-phase bcc structures with hardnesses of 4.5 GPa and 5.3 GPa and high yield strength up to 1873 K, however they are brittle at room temperature. These high melting temperatures combined with the expected phase stability over large temperature ranges makes experimental study of the thermodynamic properties of these alloys problematic, as it is unlikely that thermodynamic equilibrium can be achieved on experimental time scales. Accordingly, only high-temperature (>2000 K) phase diagrams exist for the refractory

metal binaries, all of which present a single A2 phase across the entire composition range, with liquidus and solidus lines nearly coincident. Due to the lack of equilibration, what experimental evidence of thermodynamic properties at low temperatures exists is of doubtful accuracy. To study phase stability of such alloys, first-principles calculations are the most accurate method currently available.

In this study, we are interested in the possibility of the A2 phase transitioning to B2 as temperature decreases. In a previous paper,<sup>7</sup> we developed a hybrid Monte Carlo/molecular dynamics (MC/MD) method that produced such a phase transition. Based on similar atomic radii and electronegativity, we found that Mo-Nb-Ta-W orders as a pseudobinary system consisting of Group 5 (Ta,Nb) and Group 6 (W,Mo) atoms, with intergroup bonding stronger than intragroup. In this article, we propose an effective Hamiltonian that exhibits an A2–B2 transition, while showing deviations from this pseudobinary model.

### **$T = 0$ K BINARY ENTHALPIES OF FORMATION**

To generate ground state structures, we use the Alloy Theoretic Automated Toolkit (ATAT)<sup>8–11</sup> a framework that iteratively generates a cluster expansion, based on *ab initio* total energies, to suggest new candidate ground state structures for a given lattice type. We applied ATAT to all six binary combinations of Mo, Nb, Ta, and W on a bcc lattice. Between 60 and 100 structures were generated per binary. The *k*-point-per-reciprocal-atom density was fixed to 9,000 for all binaries. All binaries finished with cross-validation scores less than 0.0063. Subsequent relaxation and convergence of predicted ground state and metastable structures in *k*-point density was then performed. To calculate total energies, we use the Vienna Ab Initio Simulation Package,<sup>12,13</sup> a plane-wave *ab initio* package implementing projector augmented wave pseudopotentials.<sup>14</sup> We use the Perdew–Burke–Ernzerhof (PBE) density functional,<sup>15</sup> with default energy cutoffs for total energy calculations. Relaxation was performed at  $P = 0$ . To our knowledge, no examinations of refractory metal binaries have been performed using this functional.

We identify structures by the notation [chemical formula].[Pearson symbol], using only the Pearson symbol when the chemical formula is implicitly understood. Common candidate structures for these binaries include cP2 at 50% composition (Strukturbericht B2, prototype CsCl), oA12 at 50% composition (Strukturbericht B2<sub>3</sub>), tI6 at 33.3% and 66.7% compositions (Strukturbericht C11<sub>b</sub>, prototype MoSi<sub>2</sub>), and cF16 at 25% and 75% compositions (Strukturbericht D0<sub>3</sub>, prototype BiF<sub>3</sub>). oA12, a variant of cP2 with antiphase boundaries, is of special importance as it has been identified by previous work<sup>16,17</sup> using cluster expansion methods as a potential ground state structure in Mo-Nb, Nb-W, and Ta-W.

Our results for binaries (Fig. 1) may be summarized as follows. Mo-Ta shows strongest bonding, with strongest enthalpy of formation of  $-186$  meV/atom. Mo-Nb and Ta-W have nearly equal bonding at  $-103$  meV/atom and  $-110$  meV/atom, respectively, with Nb-W the weakest of the intergroup binaries at  $-53$  meV/atom. The intragroup binaries Mo-W and Nb-Ta are essentially ideal (i.e., vanishing enthalpy). This ordering is consistent with electronegativity and atomic radii differences.<sup>7</sup> Mo-Ta and Mo-Nb have roughly symmetric convex hulls about equiatomic concentration, whereas Nb-W and Ta-W are biased toward high W concentrations with minima at 66.7% W. Both sets of observations are consistent with experimental observations that intergroup alloys Mo-Ta, Mo-Nb, Nb-W, and Ta-W exhibit cleavage near equiatomic concentrations, whereas Mo-W and Nb-Ta exhibit flow.<sup>18</sup> We confirm that in these systems, cP2 is not the stable structure at equiatomic concentration, with the exception of Mo-W where enthalpies of formation deviate negligibly from ideality, and that oA12 is stable for many of the binaries. However, with the exception of Nb-W, cP2 is within 10 meV/atom of the convex hull. This suggests that a B2 phase could be stabilized at intermediate temperature through the entropy of intragroup mixing. Below we compare our predictions for individual binaries with prior literature.

#### **Mo-Nb**

Previous first-principles calculations on this system have been performed by Curtarolo et al.<sup>20</sup> and Blum and Zunger.<sup>17</sup> Although both observe cP2, Mo-rich cF16, and Mo-rich and Nb-rich tI6 structures stable using the local density approximation (LDA) functional, Blum and Zunger contended that their mixed-basis cluster expansion (MBCE) fit indicates that cP2 and Nb-rich tI6 are not stable and that at equiatomic concentration, oA12 is stable (although LDA predicts this structure to be unstable). Our PBE study predicts oA12 is stable and minimizes the enthalpy of formation at  $-102.9$  meV/atom, while cP2 lies 4.3 meV/atom above. We find both Mo-rich and Nb-rich tI6 lie on the convex hull. Mo-rich cF16 lies 1.0 meV/atom off the convex hull, well within margin of error, but Ta-rich cF16 lies substantially above at 18.9 meV/atom. The Mo-rich side of the convex hull is more detailed than the Nb-rich side, although the convex hull is generally symmetric about equiatomic concentration.

#### **Mo-Ta**

Previous first-principles work on this system has been performed on this system by Blum and Zunger<sup>17,21</sup> and Turchi et al.<sup>22</sup> While Blum and Zunger observed cP2 and Mo-rich and Ta-rich tI6 to be stable using the LDA functional, their MBCE stated that Ta-rich tI6 is not stable. Turchi et al., using a cluster variation method approach combined with first-principles calculations, found an A2 to B2

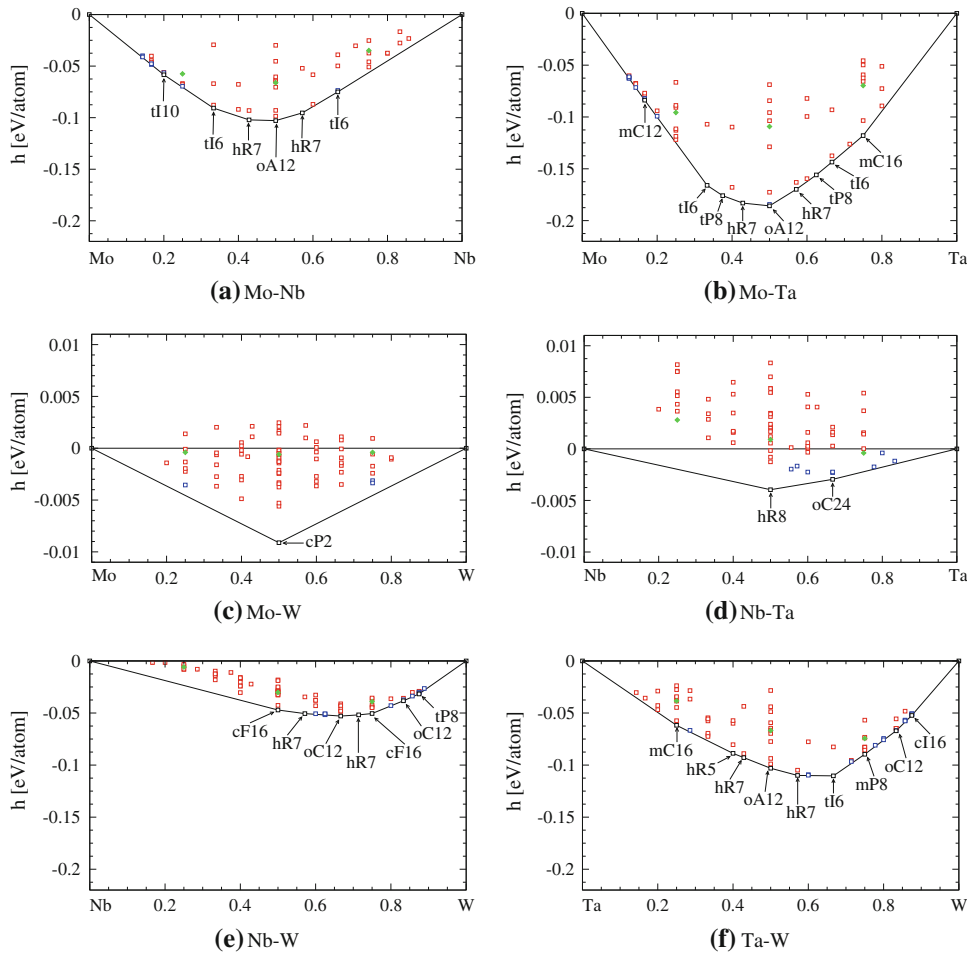


Fig. 1. First-principles enthalpies of formation for binaries. Black squares denotes structures on the convex hull, blue squares denotes structures within 2 meV/atom of the convex hull, and red squares above 2 meV/atom. The filled green diamonds denote 16-atom bcc SQS structures.<sup>19</sup> The scales of Mo-W and Nb-Ta differ from the scales from the other four binaries.

transition at 1772 K and 47% Ta. oA12 minimizes enthalpy of formation for the system at  $-185.8$  meV/atom, with cP2 1.4 meV/atom above. We find Mo-rich and Ta-rich tI6 to both be stable, in agreement with LDA results but not Blum and Zunger's MBCE. van Torne and Thomas<sup>18</sup> observed nonideal behavior in Mo-Ta bcc solid solutions at  $T = 273$  K, in line with the tendency toward chemical ordering, although they attribute this to concentration gradients in their sample that were likely not in equilibrium.

### Mo-W and Nb-Ta

For binaries Mo-W and Nb-Ta, at 2000 K and 2600 K, respectively, experimental enthalpies of mixing are low for all compositions, and activities perfectly follow Raoult's law, suggesting an ideal solution with no chemical bonding. This is in agreement with our first-principles calculations, which have a minimum enthalpy of formation of  $-10$  meV/atom and  $-3$  meV/atom for Mo-W and Nb-Ta, respectively, indicating nearly perfect mixing of

atomic species. This is in agreement with Villar's empirical criteria,<sup>23</sup> as both binaries consist of bcc metals with similar electronegativity and atomic radius. To our knowledge, no other first-principles results for these binaries exist in the literature.

### Nb-W

For Nb-W, significant deviations from symmetry in the convex hull are observed, with no stable structures found on the Nb-rich side of the convex hull. The equiatomic concentration stable structure is cF16 (prototype NaTl), with cP2 28.2 meV/atom above. However, the minimum enthalpy of formation structure is an oC12 structure at 66.7% W with enthalpy of formation at  $-52.9$  meV/atom. Blum and Zunger<sup>17</sup> also found a detailed W-rich side of the convex hull and a Nb-rich side containing only one structure that negligibly affects the shape of the convex hull. In particular, our PBE predicts W-rich tI6 is unstable by 6.6 meV/atom, which does not agree with LDA results but does agree with Blum and Zunger's MBCE.

## Ta-W

Of all binaries considered, Ta-W is the most studied. Experimental work<sup>24</sup> indicated a negative deviation from Vegard's law for lattice constants, asymmetry of the enthalpy of mixing toward the Ta-rich side, and significant deviation from ideality of activities at 1200 K, suggesting the presence of short-range order. Early work by Turchi et al.<sup>25</sup> focused only on cP2 and cF16, both Ta- and W-rich, finding all three structures stable. Order-disorder transitions were studied by Masuda-Jindo et al.<sup>26</sup> using a cluster expansion fitted from first-principles calculations on random alloys, finding a second-order A2 to B2 phase transition first appearing around 1000 K at near equiatomic concentration. We find oA12 to be stable at equiatomic concentration at an enthalpy of formation of  $-103.1$  meV/atom, with cP2  $9.4$  meV/atom above, but W-rich tI6 minimizes enthalpy of formation at  $-110.3$  meV/atom. That the convex hull leans W-rich is supported by the cluster expansions of Blum and Zunger et al.<sup>17</sup> and Hart et al.,<sup>16</sup> both of whose cluster expansions have W-rich tI6 on the convex hull and nearly minimizing the enthalpy of formation. Although the convex hull leaning W-rich disagrees with experimental evidence, this is in line with other theoretical results, and at 1200 K it is unlikely that experimental results can be properly equilibrated.

## QUATERNARY AND MC/MD RESULTS

By the third law of thermodynamics, at  $T = 0$  K we expect Mo-Nb-Ta-W to chemically order or to phase segregate into well-ordered structures. Considering only binary structures, we find at the equiatomic concentration for Mo-Nb-Ta-W the stable coexisting phases are MoTa.oA12, NbW.cF16, TaW<sub>2</sub>.tI6, and Mo<sub>3</sub>Nb<sub>4</sub>.hR7, with an average enthalpy of formation of  $-117$  meV/atom. That the first three are stabilized in the quaternary is not surprising as they are the enthalpy-minimizing structures in their respective binaries. MoTa.oA12 in particular is stabilized as it has an enthalpy of formation a factor of 2 or more larger than all other binaries. While MoNb.oA12 is the enthalpy of formation minimizing structure for Mo-Nb, the convex hull for the Mo-Nb system is shallow at near equiatomic concentration, and thus little enthalpy is lost segregating out Mo<sub>3</sub>Nb<sub>4</sub>.hR7 instead. This allows TaW<sub>2</sub>.tI6 and NbW.cF16 to be stabilized while maintaining the proper stoichiometry.

In this article, we examine our previously reported MC/MD calculations<sup>7</sup> in Mo-Nb-Ta-W in light of the  $T = 0$  K binary phase diagrams. As previously reported and reproduced in this article, the nearest-neighbor partial distribution functions (NN-PDFs) at  $T = 300$  K in Fig. 2 generally agree with the magnitudes of enthalpies obtained from the previous section, although deviations exist. Mo-Ta has the largest enthalpy of formation, and indeed the NN-PDF for Mo-Ta shows the strongest peak, suggesting enthalpic

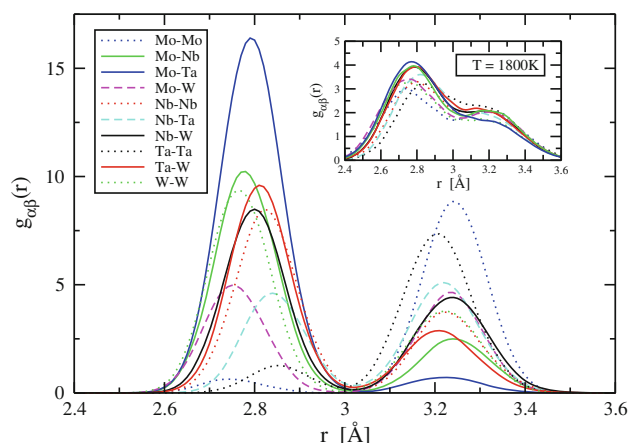


Fig. 2. Partial density functions obtained from MC/MD for the Mo-Nb-Ta-W bcc phase, showing first and second nearest neighbors. The solid lines denote PDFs between species from differing groups, and the dashed lines between differing species from the same group, and dotted lines between the same species. The main figure shows results for  $T = 300$  K, and the inset for  $T = 1800$  K.

stabilization. Next comes Nb-Mo and Ta-W, which are nearly degenerate in enthalpy, and their NN-PDFs are nearly equal. Nb-Nb and W-W come next, which anomalously deviate from pseudobinary behavior, as they are intragroup peaks. Nb-W is the weakest of the intergroup bonds and has the smallest NN peak, although it is still significant. The remainder are all intragroup, with the NN peaks for Mo-Mo and Ta-Ta at nearly zero. As a possible explanation for the presence of W-W and Nb-Nb NN bonds, note that at  $T = 0$  K, two of the stable structures near this stoichiometry, TaW<sub>2</sub>.tI6 and Mo<sub>3</sub>Nb<sub>4</sub>.hR7, are W-rich and Nb-rich, respectively, yielding W-W and Nb-Nb bonds. The anomalous NN peaks may indicate the tendency of the system to undergo partial phase segregation at this temperature. The next-nearest-neighbor partial distribution functions (NNN-PDFs) at  $T = 300$  K show exactly opposite ordering, with Mo-Mo and Ta-Ta showing strong peaks and Mo-Ta essentially zero, characteristic of cP2-like ordering.

For  $T = 1800$  K, shown in the inset of Fig. 2, all NN peaks have similar magnitude, as do NNN peaks. By  $T = 1800$  K, ordering has apparently been lost and the system is a random bcc solid solution. We propose the following temperature evolution. At a high temperature, the system is a nearly ideal disordered bcc solution, as shown by the  $T = 1800$  K PDF. As the temperature of the system decreases, the system undergoes an order/disorder phase transition, most likely to cP2-like alternation with the pattern of chemical order reflecting preferred bonding types among species. As the temperature further decreases, additional phase transitions are possible, culminating in phase segregation into the  $T = 0$  K coexisting phases.

## A FREE ENERGY MODEL FOR Mo-Nb-Ta-W

To calculate qualitative details of the order-disorder transition in Mo-Nb-Ta-W, we derive a mean

field free energy model for chemical ordering within the bcc phase. Previous work on phase stability using MC methods has been performed by del Grosso et al.<sup>27,28</sup>; however, their empirical interaction model predicts Mo and Ta avoid NN bonding at  $T = 0$  K. This yields different low-temperature phase segregation behavior than what first principles unambiguously predicts. As we are using a mean field model, local elastic distortion of the crystal lattice due to atomic radius mismatch, a known strong effect in HEAs,<sup>29</sup> is incorporated in our study only insofar as it affects the binary enthalpies of formation.

We work in the Gibbs ensemble at fixed temperature, pressure, and chemical composition in a system with  $N$  atoms and  $d$  chemical species, all of which have the same number of atoms  $N/d$ . We consider only nearest-neighbor interactions, which for a bcc lattice exist between cell center and cell vertex sites, yielding an enthalpy in the form of an effective Hamiltonian

$$H = \sum_{\langle ij \rangle} \sum_{\alpha\beta} \sigma_\alpha(i) b_{\alpha\beta} \sigma_\beta(j) \quad (1)$$

where  $i$  and  $j$  denotes all possible sites, summation over  $\langle ij \rangle$  denotes summation over all nearest-neighbor bonds, summation over  $\alpha$  and  $\beta$  denotes summation over all possible species,  $b_{\alpha\beta}$  denotes the nearest-neighbor bond strength between species  $\alpha$  and  $\beta$ , and  $\sigma_\alpha(i)$  is 1 if site  $i$  contains species  $\alpha$  and 0 otherwise.

Anticipating cP2-like ordering, we now define the quantities

$$e_\alpha = \frac{2}{N} \sum_{i \in \text{vertices}} \sigma_\alpha(i) \quad (2)$$

and

$$o_\alpha = \frac{2}{N} \sum_{i \in \text{centers}} \sigma_\alpha(i) \quad (3)$$

which are, respectively, the concentration of species  $\alpha$  on cell vertex (“even”) sites and the concentration of species  $\alpha$  on cell center (“odd”) sites. Inverting Eqs. 2 and 3, we rewrite  $\sigma_\alpha(i)$  as

$$\sigma_\alpha(i) = (e_\alpha, o_\alpha) + \delta\sigma_\alpha(i) \quad (4)$$

where the first term is  $e_\alpha$  if  $i$  is a cell vertex and  $o_\alpha$  if  $i$  is a cell center. As all NN bonds are between cell centers and vertices, we may rewrite Eq. 1 as

$$H = \sum_{i \in \text{centers}} \sum_{j \in \text{NN}(i)} \sum_{\alpha\beta} (o_\alpha + \delta\sigma_\alpha(i)) b_{\alpha\beta} (e_\beta + \delta\sigma_\beta(j)) \quad (5)$$

In a mean field approximation, the terms in  $\delta\sigma$  vanish. The remaining term is independent of  $i$  and  $j$  and thus scales as the total number of bonds  $4N$ , giving an enthalpy per atom of

$$h = H/N = \sum_{\alpha\beta} o_\alpha \Omega_{\alpha\beta} e_\beta \quad (6)$$

where  $\Omega_{\alpha\beta} = 4b_{\alpha\beta}$ .

We now introduce the ideal entropy approximation, assigning an entropy per atom of

$$s = -\frac{k_B}{2} \sum_\alpha (e_\alpha \ln(e_\alpha) + o_\alpha \ln(o_\alpha)) \quad (7)$$

As  $e_\alpha$  and  $o_\alpha$  are bounded between 0 and  $2/d$  and sum to 1, this entropy can only vanish in the case where  $d = 2$ , whereas we will apply this free energy to HEAs with  $d > 3$ . Hence, this entropy violates the third law of thermodynamics if we were to naively extrapolate it to  $T = 0$  K. This is a natural consequence of B2 ordering, with two unique sites occupied by  $d > 2$  chemical species, requiring disorder on the sites and creating entropy of mixing. To predict phase transitions at lower temperatures, both a unit cell with number of unique sites divisible by 4, and more interaction terms, must be included. Including the entropic contribution  $-Ts$ , we obtain a free energy per atom of

$$g = \sum_{\alpha\beta} o_\alpha \Omega_{\alpha\beta} e_\beta + \frac{k_B T}{2} \sum_\alpha (e_\alpha \ln(e_\alpha) + o_\alpha \ln(o_\alpha)) \quad (8)$$

We now examine ordering tendencies driven by the energetics of the system. Suppose we have an enthalpy of general quadratic form

$$h = \psi^T \Omega \psi \quad (9)$$

where  $\psi$  is a vector containing  $n + r$  variables, where  $n$  of the variables are independent and  $r$  are dependent, and  $\Omega$  is an  $(n + r) \times (n + r)$  dimensional symmetric matrix. We rewrite this enthalpy in terms of only independent variables. Define  $\psi$  with the first  $n$  entries independent, so that it may be decomposed into an  $n$ -dimensional vector  $\psi_i$  containing independent variables and an  $r$ -dimensional vector  $\psi_d$  containing dependent variables. Rewrite Eq. 9 in block diagonal form

$$h = \begin{bmatrix} \psi_i^T & \psi_d^T \end{bmatrix} \begin{bmatrix} \Omega^{ii} & \Omega^{id} \\ (\Omega^{id})^T & \Omega^{dd} \end{bmatrix} \begin{bmatrix} \psi_i \\ \psi_d \end{bmatrix} \quad (10)$$

where  $\Omega^{ii}$  is an  $n \times n$  dimensional matrix,  $\Omega^{id}$  an  $n \times r$  matrix, and  $\Omega^{dd}$  and  $r \times r$  matrix. Assume that  $\psi_d$  depends linearly on  $\psi_i$ , so the constraints on the system may be written in form

$$\psi_d = \mathbf{k} + D\psi_i \quad (11)$$

with  $\mathbf{k}$  an  $r$ -dimensional vector and  $D$  an  $r \times n$  dimensional matrix. Imposing this on Eq. 10 yields

$$h = \psi_i^T \theta \psi_i + B\psi_i + C \quad (12)$$

where  $\theta = \Omega^{ii} + \Omega^{id}D + D^T(\Omega^{id})^T + D^T\Omega^{dd}D$  is an  $n \times n$  matrix,  $B = 2\mathbf{k}^T((\Omega^{id})^T + \Omega^{dd}D)$  a  $n$ -dimensional row vector, and  $C = \mathbf{k}^T\Omega^{dd}\mathbf{k}$ . If  $\theta$  is invertible, then  $h$  has a unique extremum at

$$\psi_0 = -\frac{1}{2}\theta^{-1}B^T \quad (13)$$

so Eq. 12 may be rewritten with a coordinate redefinition of  $\psi' = \psi - \psi_0$  as

$$h = \psi'^T\theta\psi' + C - \psi_0^T\theta\psi_0 \quad (14)$$

As  $\Omega^{ii}$  and  $\Omega^{dd}$  are symmetric,  $\theta$  must be a real symmetric matrix and is therefore diagonalizable with orthogonal eigenvectors. Its eigenvalues and eigenvectors yield information about preferential ordering in the system.

Returning to the special case of cP2 symmetry, there are  $d$  constraints of the form

$$e_\alpha + o_\alpha = \frac{2}{d} \quad (15)$$

one for each  $\alpha$ , and two constraints imposing that each site class must be completely occupied:

$$\sum_\alpha e_\alpha = \sum_\alpha o_\alpha = 1 \quad (16)$$

However, the two constraints of Eq. 16 are redundant, as required by Eq. 15. It follows that only  $d - 1$  of the original  $2d$  variables are independent. Here, we take all  $o_\alpha$  and one of the  $e_\alpha$  to be dependent. For cP2 ordering, translational symmetry and equiatomic composition require all components of  $\psi_0$  equal  $1/d$ . This yields an enthalpy of the form

$$h = \sum_{\alpha'\beta'} \left(e_{\alpha'} - \frac{1}{d}\right)\theta_{\alpha'\beta'} \left(e_{\beta'} - \frac{1}{d}\right) + \frac{1}{d^2} \sum_{\alpha\beta} \Omega_{\alpha\beta} \quad (17)$$

where primed indices denote summation over independent species and unprimed indices denote summation over all species. The enthalpy is invariant under the body-centering operation  $e_\alpha \rightarrow 2/d - e_\alpha$ . This enthalpy has the natural form expected for an order-disorder transition. In particular, for the binary ( $d = 2$ ) system A–B,  $h = \Omega_{AB}(e_A - \frac{1}{2})^2$  up to a constant, with  $e_A - \frac{1}{2}$  the well-known order parameter for the order/disorder phase transition in the cP2 structure.

We diagonalize  $\theta$ , obtaining its eigenvectors  $\mathbf{v}_i$  with associated eigenvalues  $\lambda_i$ . Any point in composition space may be written as  $\psi' = \sum_i \chi_i \mathbf{v}_i$ , where  $\chi_i$  is the associated normal coordinate for eigenvector  $\mathbf{v}_i$ . Each normal coordinate is a linear combination of  $e_\alpha$ 's, with  $\chi_i = 0 \forall i$  corresponding to  $e_\alpha = \frac{1}{d} \forall \alpha$ . Normalizing the eigenvectors with a magnitude of unity, the enthalpy becomes

$$h = \sum_i \lambda_i \chi_i^2 + \frac{1}{d^2} \sum_{\alpha\beta} \Omega_{\alpha\beta} \quad (18)$$

There are two cases for the temperature evolution of the system, depending on the spectrum of  $\theta$ . In the first case,  $\theta$  has only positive or zero eigenvalues. In this case, the enthalpy-minimizing configuration is  $\chi_i = 0 \forall i$ . As this is also the entropy maximizing configuration, the system remains disordered at  $e_\alpha = 1/d \forall T$ . No order/disorder phase transition occurs if  $\theta$  has only non-negative eigenvalues.

In the second case,  $\theta$  has negative eigenvalues leading to solutions with enthalpy less than the disordered solution. Were it not for the constraint  $0 \leq e_\alpha \leq 2/d$ , the enthalpy would be unbounded below. The  $T = 0$  K enthalpy-minimizing solution must lie on the boundary of configuration space, i.e.,  $e_\alpha = 0$  or  $e_\alpha = 2/d$  (which are physically equivalent due to body centering symmetry) for at least one species  $\alpha$ , corresponding to at least one species showing perfect ordering at  $T = 0$  K. At any point in configuration space not on the boundary, we may always increase the normal coordinate corresponding to any negative eigenvalue to lower the enthalpy until the boundary is reached. In general, multiple normal coordinates contribute to the solution. Nonzero normal coordinates for positive eigenvalues may exist, as increasing the normal coordinates for positive eigenvalues may move the system in configuration space away from the boundary. Subsequently increasing the normal coordinate for negative eigenvectors moves the system in configuration space back to the boundary, possibly with lower enthalpy than before. As the enthalpy is independent of temperature, there must be a finite temperature where the entropic contribution to free energy (which grows proportionate to  $T$ ) dominates the enthalpic contribution. An order/disorder phase transition must occur if  $\theta$  has at least one negative eigenvalue.

## RESULTS OF FREE ENERGY MODEL

To determine whether an order-disorder phase transition exists in Mo-Nb-Ta-W, we compute the NN bond strengths  $b$ . Using the structures previously obtained from ATAT, we reran the cluster expansion, restricting it to a single two-body term, which yields the NN bond strengths between differing species given in Table I. Shown in Table II are the eigenvalues of the  $\theta$  matrix, the eigenvectors, and the associated dependent composition  $e_{\text{Mo}} - 1/d = \sum_{\alpha'} (e_{\alpha'} - 1/d)$ .

Positive signs for eigenvector components denote ordering on cell vertices and negative signs denote ordering on cell centers (only the relative sign between components are relevant). Of the three possible modes, one has a negative eigenvalue, so an order/disorder phase transition must exist. The lowest enthalpy mode ordering the system ( $\lambda = -701$  meV/atom) indeed has strong ordering with opposite signs for Mo and Ta, supporting the assertion that Mo-Ta NN bonds drive the ordering

**Table I. Nearest-neighbor bond strengths  $B$  used in modeling the Mo-Nb-Ta-W BCC phase, in units of MeV/atom**

	Group 5		Group 6	
	Ta	Nb	W	Mo
Ta	0	1	-34	-53
Nb	1	0	-14	-30
W	-34	-14	0	-1
Mo	-53	-30	-1	0

**Table II. The Eigenvalues and associated Eigenvectors of  $\theta$  using bond strengths given in Table I**

$\lambda$	$e_{\text{Ta}}-1/4$	$e_{\text{Nb}}-1/4$	$e_{\text{W}}-1/4$	$e_{\text{Mo}}-1/4$
-701	0.786	0.600	0.152	-1.537
8	0.321	-0.186	-0.929	0.793
18	-0.529	0.778	-0.339	0.089

$\lambda$  is in units of meV/atom. The final column is the selected dependent species and is not part of the associated eigenvector; it is shown here to give physical intuition to how the particular mode is ordering the system.

of the system. This mode also has strong ordering with opposite signs on Mo and Nb, in agreement with Mo-Nb as the second strongest bonding type.

Shown in Fig. 3 is the temperature evolution of the species concentration on cell vertices, obtained by minimizing the free energy at a given temperature over all independent variables  $e_{\alpha'}$  subject to the bounds. MC simulations using the same enthalpy model were subsequently performed to verify our mean field results, and they show excellent qualitative agreement. Here, the system achieves perfect sublattice occupancies for all species at low temperature, with Ta and Nb on the cell vertices and W and Mo on the cell centers. This agrees with our pseudobinary model where Group 5 (Ta,Nb) and Group 6 (W,Mo) form pseudobinary species. As the temperature increases, the system begins picking up some disorder, with Nb and W more strongly affected than Mo and Ta, finally reaching complete disorder at  $T_C = 1654$  K. Our MC simulations predict  $T_C = 1280$  K, less than the mean field value, as expected. The temperature evolution of the enthalpy of this model (not shown) shows monotonic behavior up to the transition temperature, suggesting a second-order transition.

The inset shows the temperature evolution of the quantities  $e_{\text{Ta}} + e_{\text{Mo}}$  and  $e_{\text{Nb}} + e_{\text{W}}$ , both quantities remaining close to  $1/2$  for all temperatures, explaining the mirror-image-like relation of Mo to Ta and Nb to W. This arises from Mo-Ta's strong binding, pinning the configuration close to the boundary  $e_{\text{Ta}} \approx e_{\text{Nb}} \lesssim \frac{1}{2}$ , with  $e_{\text{W}} \approx e_{\text{Mo}} \gtrsim 0$  at low temperatures. Even at  $T \approx 1000$  K, where  $e_{\text{Nb}}$  and  $e_{\text{W}}$  differ appreciably from their boundary values,  $e_{\text{Ta}}$  and  $e_{\text{Mo}}$  remain close to their extremes, requiring that  $e_{\text{Nb}} + e_{\text{W}} = 1 - (e_{\text{Ta}} + e_{\text{Mo}}) \approx \frac{1}{2}$ . By the time

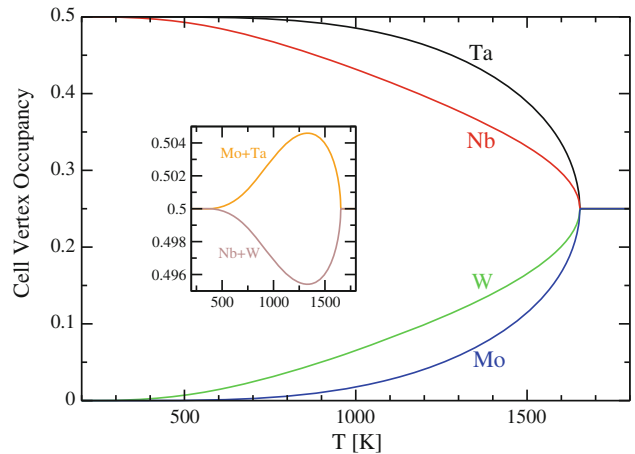


Fig. 3. The vertex sublattice occupancy as a function of temperature. See text for information on inset.

$T$  reaches  $T_C$ ,  $e_{\alpha} = \frac{1}{4} \forall \alpha$ , so the values of  $e_{\text{Ta}} + e_{\text{Mo}}$  and  $e_{\text{Nb}} + e_{\text{W}}$  never deviate significantly from  $1/2$ .

Figure 4 shows the temperature evolution of the normal coordinates of the system. At low temperatures, all modes contribute to the thermodynamic equilibrium of the system, although the  $-701$  meV/atom mode dominates the enthalpy of the system. All three normal coordinates vanish at  $T_C = 1654$  K, yielding the disordered solution where entropy is maximized in configuration space. The square root singularity as  $T \rightarrow T_C$  matches the well-known mean field classical critical exponent  $\beta = \frac{1}{2}$ .

The system strongly prefers the  $-701$  meV/atom mode at  $T = 0$  K due to its substantially low enthalpy. This places Ta, Nb, and W on cell vertices

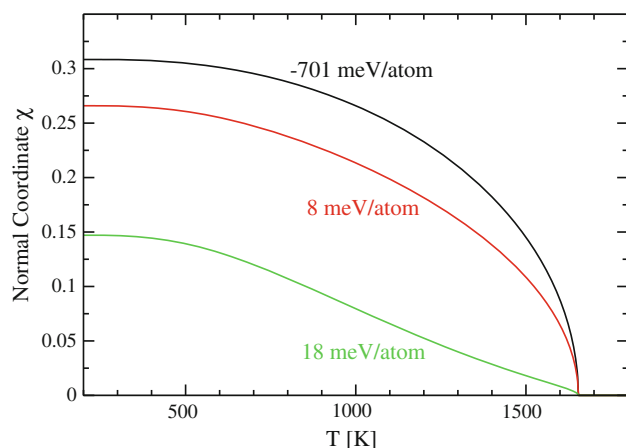


Fig. 4. The normal coordinates of the system as function of temperature.

and Mo on cell centers. To maintain overall concentration 1/4 for each species, the other two modes are needed to compensate. The 8 meV/atom mode replaces some Mo at cell centers with W, while further strengthening the ordering of Ta on cell vertices. Finally, the least favored 18 meV/atom mode is the only mode that orders Nb and W onto different sublattices, giving the observed disordering of Nb and W in Fig. 3. The large contribution of Mo-Ta ordering in the  $-701$  meV/atom mode presents compelling evidence of ordering dominated by Mo-Ta bonding.

## CONCLUSIONS

In summary, we apply mean field theory to a first-principles-based effective Hamiltonian to examine the possibility of chemical ordering in equiatomic Mo-Nb-Ta-W. Within the confines of our near-neighbor interaction model, we predict the emergence of a B2 type alternation of occupation probability on a body-centered cubic (A2 type) lattice. A mixture of Ta and Nb predominates on one site class (e.g., even sites), alternating with a mixture of Mo and W on the other site class (e.g., odd sites). This ordering occurs through a continuous phase transition at  $T_C = 1654$  K within the mean field approximation.

Longer-range interactions not included in our near-neighbor model can interrupt the B2-type order. For example, in the strongly binding Mo-Ta binary, the energetically favorable structure is Pearson type oA12 (Strukturbericht B23), which places antiphase boundaries every third (110)

plane.<sup>17</sup> As the perfectly ordered B2 structure lies only 1.4 meV/atom higher in energy, this distinction should only be relevant at very low temperatures. However, our first-principles calculations predict low-temperature-phase segregation into a mixture of binary phases. Our mean field theory is therefore intended to be applied at high temperatures in the chemically disordered or weakly ordered regimes.

## REFERENCES

1. R. Kozak and W. Steurer, *Intermetallics* (2013) (submitted).
2. J.-W. Yeh, S.-K. Chen, S.-J. Lin, J.-Y. Gan, T.-S. Chin, T.-T. Shun, C.-H. Tsau, and S.-Y. Chang, *Adv. Eng. Mater.* 6, 299 (2004).
3. J.-W. Yeh, S.-K. Chen, J. Gan, S.-J. Lin, T.-S. Chin, T.-T. Shun, C.-H. Tsau, and S.-Y. Chang, *Metall. Mater. Trans. A* 35A, 2533 (2004).
4. Y.J. Zhou, Y. Zhang, Y.L. Wang, and G.L. Chen, *Appl. Phys. Lett.* 90, 181904 (2007).
5. O.N. Senkov, G.B. Wilks, D.B. Miracle, C.P. Chuang, and P.K. Liaw, *Intermetallics* 18, 17581765 (2010).
6. O.N. Senkov, G.B. Wilks, J.M. Scott, and D.B. Miracle, *Intermetallics* 19, 698 (2011).
7. M. Widom, W.P. Huhn, S. Maiti, and W. Steurer, *Metall. Mater. Trans. A* (2013). doi:10.1007/s11661-013-2000-8.
8. A. van de Walle and G. Ceder, *J. Phase Equilib.* 23, 348 (2002).
9. A. van de Walle and M. Asta, *Model. Simul. Mater. Sci.* 10, 521 (2002).
10. A. van de Walle, M. Asta, and G. Ceder, *CALPHAD* 26, 539 (2002).
11. A. van de Walle, *CALPHAD* 33, 266 (2009).
12. G. Kresse and J. Hafner, *Phys. Rev. B* 43, 558 (1993).
13. G. Kresse and J. Furthmüller, *Phys. Rev. B* 54, 11169 (1996).
14. P.E. Blöchl, *Phys. Rev. B* 50, 17953 (1994).
15. J.P. Perdew, K. Burke, and M. Ernzerhof, *Phys. Rev. Lett.* 77, 3865 (1996).
16. G.L.W. Hart, V. Blum, M.J. Malorski, and A. Zunger, *Nat. Mater.* 4, 391 (2005).
17. V. Blum and A. Zunger, *Phys. Rev. B* 72, 020104 (2005).
18. L.I. van Torne and G. Thomas, *Acta Metall. Mater.* 14, 621 (1966).
19. C. Jiang, C. Wolverton, J. Sofo, L.-Q. Chen, and Z.-K. Liu, *Phys. Rev. B* 69, 214202 (2004).
20. S. Curtarolo, D. Morgan, and G. Ceder, *CALPHAD* 29, 163 (2005).
21. V. Blum and A. Zunger, *Phys. Rev. B* 69, 020103 (2004).
22. P.E.A. Turchi, V. Drchal, J. Kudrnovský, C. Colinet, L. Kaufman, and Z.-K. Liu, *Phys. Rev. B* 71, 094206 (2005).
23. P. Villars, *J. Less-Common Met.* 92, 215 (1983).
24. S.C. Singhal and W.L. Worrell, *Metall. Trans.* 4, 895 (1973).
25. P.E.A. Turchi, A. Gonis, V. Drchal, and J. Kudrnovský, *Phys. Rev. B* 64, 085112 (2001).
26. K. Masuda-Jindo, V.V. Hung, N.T. Hoa, and P.E.A. Turchi, *J. Alloy. Compd.* 452, 127 (2008).
27. M.F. del Grosso, G. Bozzolo, and H.O. Mosca, *Physica B* 407, 3285 (2012).
28. M.F. del Grosso, G. Bozzolo, and H.O. Mosca, *J. Alloy. Compd.* 534, 25 (2012).
29. Y. Zhang, Y.J. Zhou, J.P. Lin, G.L. Chen, and P.K. Liaw, *Adv. Eng. Mater.* 10, 534 (2008).